BEAMWIDTH AND DIRECTIVITY OF LARGE SCANNING ARRAYS*

R. S. ELLIOTT
PROFESSOR OF ENGINEERING
UNIVERSITY OF CALIFORNIA AT LOS ANGELES
Los Angeles • California

First of Two Parts

INTRODUCTION

Many aspects of antenna array theory, particularly for uniform element spacing, are so widely known that they form a standard body of knowledge in textbooks.[1] In the case of linear arrays, general formulas for beamwidth and directivity have been established. However, in the case of planar arrays only the case of uniform excitation has been extensively investigated.[2,3] Surprisingly, no great advantage has been taken of the use of a Fourier series representation of the aperture distribution. Such a representation yields useful results of fairly general validity in the case of planar arrays, and even enhances the well known aspects of the linear theory. It is a purpose of the present paper to exhibit the advantages of such a representation.

LINEAR ARRAY THEORY

Pattern Shape

Consider first an array of $2N_z+1$ identical elements, symmetrically disposed along the Z axis, with common spacing d_z, as suggested by Figure 1. The conventional relation between spherical and rectangular coordinates is adopted and the far field array factor can then be written

$$A(\theta) = \sum_{n=-N_z}^{N_z} I_n e^{jn\,(kd_z\cos\theta-\alpha_z)} = \sum_{-N_z}^{N_z} f_n \qquad (1)$$

in which it has been assumed that the current distribution has a uniform progressive phase, governed by the parameter α_z, and a symmetrical amplitude distribution. Thus, $I_n =$

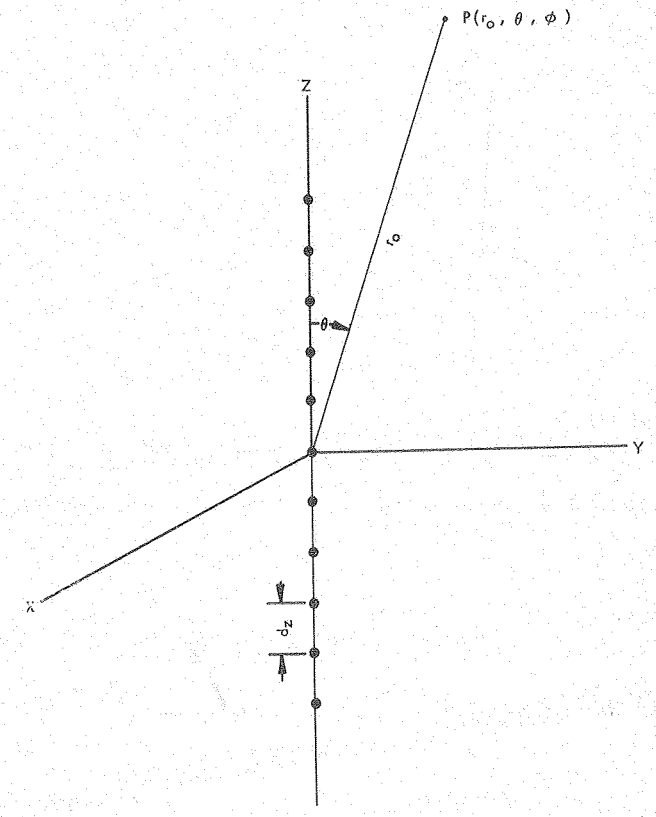

Figure 1 — Linear array geometry.

* *This study was supported under a consulting arrangement with Lockheed Aircraft Corp., Burbank, Cal.*

I_{-n} is pure real for all values of n. $k=\frac{2\pi}{\lambda}$ is the wave number.

Equation (1) can be interpreted as a symmetrical family of phasors, fanned out in the complex plane as shown in Figure 2. The separation angle between adjacent phasors is $\psi=kd_z\cos\theta-\alpha_z$, and thus varies with θ. At an angle θ_0 defined by

$$\psi=kd_z\cos\theta_0-\alpha_z=0 \qquad (2)$$

all the phasors are aligned and thus

$$A(\theta_0)=\sum_{-N_z}^{N_z} I_n \qquad (3)$$

is the maximum value of the array factor. Therefore, θ_0 defines the direction of the main beam.

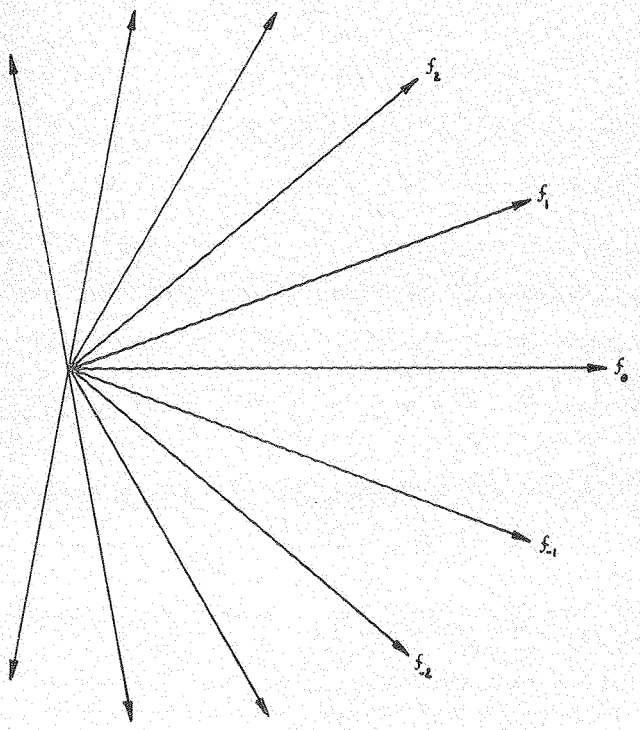

Figure 2 — Phasor representation of linear array pattern.

As θ departs from θ_0, the phasors spread out in the complex plane. For large arrays, an angle $\theta_1<\theta_0$ is reached at which the sum of the phasors is zero, defining the first null on one side of the main beam. Continuing, an angle $\theta_3<\theta_1$ is reached at which the phasors are even further spread out, and their sum is once again zero. This defines the second null on one side of the main beam. Intermediate between θ_1 and θ_3 there is an angle at which the phasors sum to a secondary maximum, defining the height of the first sidelobe. As θ is decreased still further, subsequent sidelobes and nulls are traced out.

Similarly, if θ departs in the other direction from θ_0, a sequence of angles $\theta_0<\theta_2<\theta_4<\ldots$ is reached at which array pattern nulls are obtained, with sidelobes in between. Because the array pattern is symmetrical in the variable $\psi=kd_z\cos\theta-\alpha_z$, the heights of the sidelobes on the two sides of the main beam are symmetrical also, but their positions are not necessarily symmetrical in θ. Since $A(\theta)$ is independent of ϕ, the three dimensional array pattern consists of conical lobes whose directions nest among the succession of angles $\ldots\theta_3,\theta_1,\theta_0,\theta_2,\theta_4,\ldots$

It is conceivable that the phasors of Equation (1) can spread out so far that they are once again aligned. This will occur if $kd_z\cos\theta-\alpha_z=\pm 2\pi$. If this is not to occur before the limits of real space are reached, then use of (2) establishes the conditions

$$|\cos\theta_0|+\frac{\lambda}{d_z}>1$$

$$|\cos\theta_0|-\frac{\lambda}{d_z}<-1$$

The second of these inequalities is more stringent and requires that

$$\frac{d_z}{\lambda}<\frac{1}{1+|\cos\theta_0|} \qquad (4)$$

Equation (4) is often referred to as the condition for avoidance of multiple main beams. It is a result which is independent of current distribution.* If the principal main beam is to be scanned close to endfire, so that $|\cos\theta_0|\to 1$, it is evident that the elements must be spaced only a half wavelength apart if a second main beam is to be avoided. In what follows, only linear arrays causing a single main beam will be considered.

Beamwidth

The half-power beamwidth of a linear array is defined as the angular separation between the two directions, one on each side of the main beam maximum, at which the power density is reduced by half. Let $\text{Ⓗ}=\theta'_2-\theta'_1$ be this beamwidth, in which θ'_2 and θ'_1 are the two values of θ' which satisfy the relation

$$A(\theta')=0.707\,A(\theta_0)=\sum_{-N_z}^{N_z} I_n\, e^{jn\,(kd_z\cos\theta'-\alpha_z)} \qquad (5)$$

The amplitude distribution I_n can be represented by a Fourier series, viz.,

$$I_n=\sum_{p=-P}^{P} a_p\, e^{jp\frac{2\pi n}{2N_z+1}} \qquad (6)$$

in which P is the highest spatial harmonic needed to represent the distribution. $a_p=a_{-p}$ is pure real because the distribution is symmetric. Inserting (2) and (6) in (5) gives

* *Except, of course, that the current distribution is symmetrical, and the phase is uniform progressive.*

$$A(\theta') = \sum_{-P}^{P} a_p \sum_{-N_z}^{N_z} e^{jn\, kd_z\left[\cos\theta' - \cos\theta_0 + \frac{p\lambda}{L_z}\right]}$$

$$= \sum_{-P}^{P} a_p \frac{\sin\left[\frac{2N_z+1}{2} kd_z\left(\cos\theta' - \cos\theta_0 + \frac{p\lambda}{L_z}\right)\right]}{\sin\left[\frac{1}{2} kd_z\left(\cos\theta' - \cos\theta_0 + \frac{p\lambda}{L_z}\right)\right]} \qquad (7)$$

in which $L_z = (2N_z+1)d_z$ is the length of the array. (The array length is assumed to include a distance $\frac{d_z}{2}$ beyond each end element). It is shown in Appendix A that for large arrays with conventional distributions, Equation (7) can be transformed to

$$\frac{\sin K\pi}{K\pi} = \frac{0.707}{\sum_{-P}^{P} \frac{a_p}{a_0}\left(-1\right)^{p+1} \frac{K^2}{p^2-K^2}} \qquad (8)$$

in which

$$K = \frac{L_z}{\lambda}(\cos\theta' - \cos\theta_0) \qquad (9)$$

is a substitution variable from which the beamwidth can be deduced. For small P it is a simple matter to find K from (8). Several cases will now be considered.

Case 1: Uniform Distribution

This is the simplest case of all and extremely useful as a reference. Only a_0 has a value and Equation (8) yields two solutions for K which can be written

$$\cos\theta_1' - \cos\theta_0 = 0.443\frac{\lambda}{L_z} \qquad (10)$$

$$\cos\theta_2' - \cos\theta_0 = -0.443\frac{\lambda}{L_z} \qquad (11)$$

from which it follows that the half power beamwidth is given by

$$\text{(H)} = \theta_2' - \theta_1' = \cos^{-1}\left[\cos\theta_0 - 0.443\frac{\lambda}{L_z}\right] - \cos^{-1}\left[\cos\theta_0 + 0.443\frac{\lambda}{L_z}\right] \qquad (12)$$

$$\left(0 < \theta_0 \leqslant \frac{\pi}{2}\right) \qquad (\theta_1' \geq 0)$$

As the main beam is scanned around from broadside ($\theta_0 = \frac{\pi}{2}$) to endfire ($\theta_0 = 0$), a cross-section of the beam takes on a succession of positions as indicated by Figure 3. As the conical beam closes toward endfire, a position is reached at which $\theta'_1 = 0$ and from this position to endfire, there is no half-power point on one side of the beam. For this reason $\theta'_1 = 0$ is known as the scan limit. Equation (10) will not give a real value for θ'_1 beyond this limit.

When the endfire position is reached, the concept of beamwidth once again takes on meaning. Equation (11) is still valid and one can write

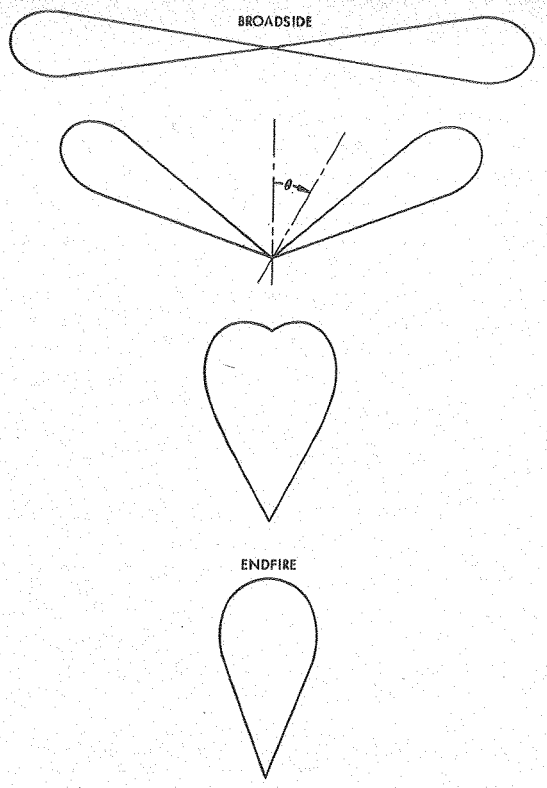

Figure 3 — Linear array pattern versus scan angle.

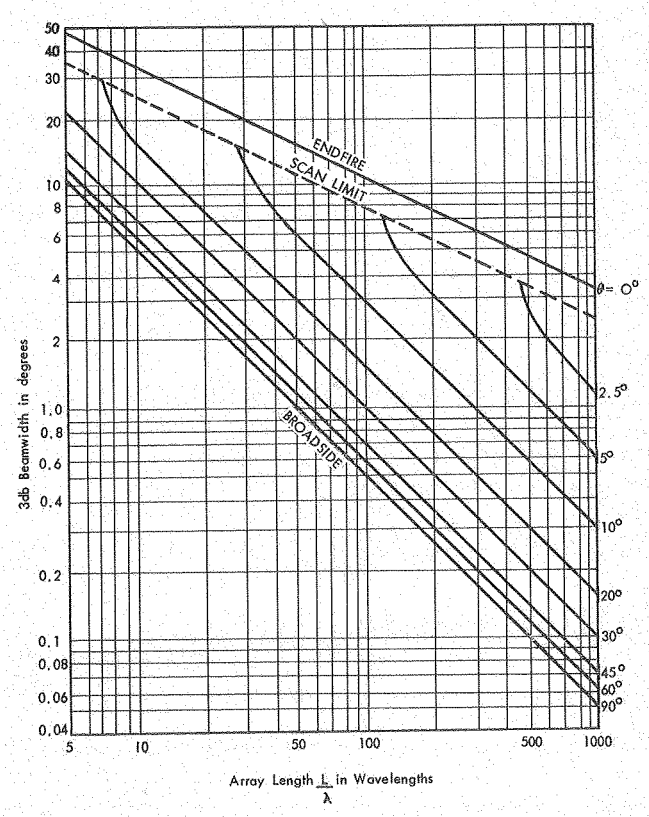

Figure 4 — Beamwidth versus linear array length and scan angle.

$$\text{(H)} = 2\theta_2' = 2\cos^{-1}\left[1 - 0.443\frac{\lambda}{L_z}\right] \qquad (13)$$

$$(\theta_0 = 0,\ \pi)$$

The beamwidths given by Equations (12) and (13) are plotted in Figure 4 as functions of array length and scan

position. These curves will prove to be useful beyond the present case of a uniform linear array, since they can be used for all the linear and planar arrays we shall discuss.

Each of these equations for beamwidth — Equation (12), which is valid to within one beamwidth of endfire, and Equation (13), which is valid at endfire — has an approximate form when $L_z >> \lambda$. Using small angle expansions, one obtains

$$\textcircled{H} \cong 0.886 \frac{\lambda}{L_z} \csc \theta_o \qquad (14)$$

(At or near broadside)

$$\textcircled{H} \cong 2 \sqrt{0.886 \frac{\lambda}{L_z}} \qquad (15)$$

(At endfire)

For $L_z > 5\lambda$, Equation (14) is in error by less than 0.2 per cent at broadside and is in error by less than 4 per cent when the beam has been scanned to within two beamwidths of endfire. For $L_z > 5\lambda$, Equation (15) is in error by less than one per cent.

Case 2: Cosine-on-a-Pedestal Distribution

For this type of excitation, Equation (8) is simply

$$\frac{\sin K\pi}{K\pi} = \frac{0.707}{1 + \frac{2a_1}{a_o} \frac{K^2}{1-K^2}} \qquad (16)$$

The range of interest is $0 \leqslant 2a_1 \leqslant a_o$ which covers the span from uniform excitation to a taper so severe that the excitation drops to zero at the ends of the array. In this span, K has an approximately parabolic dependence on taper, being given by

$$K = \pm \left[0.282 \left(\frac{2a_1}{a_o} \right)^2 + 0.443 \right] \qquad (17)$$

For the extreme taper of zero excitation at the edges ($2a_1 = a_o$), the value $K = 0.725$ agrees with other published results.[4]

For large arrays scanned not too close to endfire, Equation (17) gives for the beamwidth

$$\textcircled{H} = 0.886 \frac{\lambda}{L_z} \csc \theta_o \left[1 + 0.636 \left(\frac{2a_1}{a_o} \right)^2 \right] \qquad (18)$$

As one expects, increasing $\frac{2a_1}{a_o}$ to lower the sidelobe level has as a penalty an increase in the beamwidth. The quantity in brackets in (18) is called the beam broadening factor, f.

The radiation pattern from an equi-spaced linear array excited in a cosine-on-a-pedestal distribution consists of a main beam plus sidelobes which get successively lower as one departs in either direction from the main beam. Defining the sidelobe level as the height of the biggest sidelobe, relative to the height of the main beam, one finds by using (1) and (6), that for this case,

$$S \cong -\left[13 + 29 \left(\frac{2a_1}{a_o} \right) - 10 \left(\frac{2a_1}{a_o} \right)^2 \right] \qquad (19)$$

in which S is the sidelobe level in db. Combining (18) and (19) permits us to plot the beam broadening factor as a function of sidelobe level, as shown in Figure 5.

Case 3: Dolph-Chebyshev Distribution

It is shown elsewhere[5] that if the current distribution is chosen so that the pattern can be represented by the Chebyshev polynomial $T_{2N_z}\left(u_o \cos \frac{\psi}{2}\right)$ with ψ defined by (2), then the Fourier coefficients for such a distribution are given by

$$(2N_z+1)\, a_p = T_{2N_z}\left(u_o \cos \frac{p\pi}{2N_z+1} \right)$$

It follows that $(2N_z+1)a_o = T_{2Nz}(u_o) = r$ is the main beam to sidelobe voltage ratio. For large arrays, and for sidelobe levels in the range from -20 db to -60 db, only a_o and a_1 are significant in determining the beamwidth, and a_1 is given quite precisely by[5]

$$(2N_z+1)\, a_1 = \cosh\left[\sqrt{(\text{arc cosh } r)^2 - \pi^2} \right] \qquad (20)$$

Thus, for a Chebyshev distribution, the beamwidth can be determined as a function of sidelobe level from (18) by first finding a_1 from (20). The beam broadening factor is therefore approximately

$$f = 1 + 0.636 \left\{ \frac{2}{r} \cosh\left[\sqrt{(\text{arc cosh } r)^2 - \pi^2} \right] \right\}^2 \qquad (21)$$

Equation (21) is also plotted in Figure 5. For a linear array of any length, with the main beam pointing in any general direction, the beamwidth can be determined for a Chebyshev pattern by reading the appropriate beamwidth off Figure 4 and multiplying by the appropriate value of f, as read from Figure 5. The Chebyshev beam broadening factor of Figure 5 is in substantial agreement with the results of Stegen,[6] who used a different technique to determine the beamwidth.

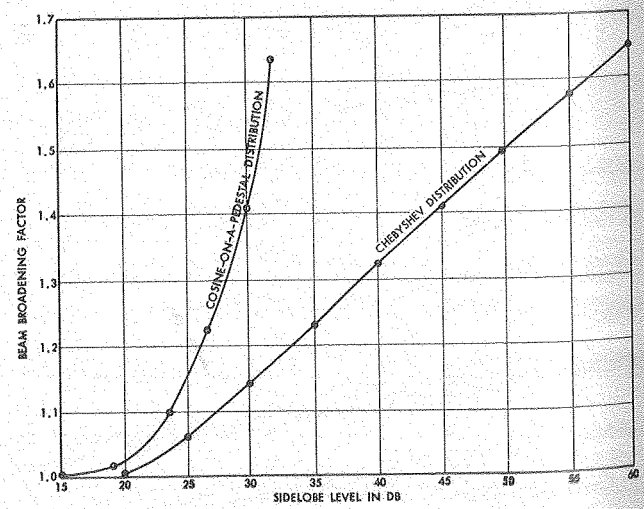

Figure 5 — Beam broadening versus side lobe level for linear arrays.

Figure 5 reveals the interesting and well-known fact that, for a given amount of beam broadening, a Chebyshev distribution is capable of yielding a lower sidelobe level than a cosine-on-a-pedestal distribution. Since only the first two Fourier terms representing the Chebyshev distribution were used in computing the Chebyshev curve in Figure 5, this result may appear paradoxical. The explanation lies in the fact that the higher Fourier terms are significant in determining sidelobe level, whereas their influence on beamwidth is slight.

Directivity

If the element pattern is isotropic, the directivity is governed entirely by the array factor. It is defined as the power density in the direction of the main beam maximum divided by the average power density from the array. Thus,

$$D=\frac{A(\theta_o)\ A^*(\theta_o)}{\frac{1}{4\pi r_o^2}\int_0^{\pi}\int_0^{2\pi} A(\theta)\ A^*(\theta)\ r_e^2 \sin\theta\ d\theta\ d\phi} \tag{22}$$

which simplifies to

$$D=\frac{2A(\theta_o)\ A^*(\theta_o)}{\int_0^{\pi} A(\theta)\ A^*(\theta)\ \sin\theta\ d\theta} \tag{23}$$

Letting $\psi=kd_z\cos\theta-\alpha_z$ so that $d\psi=-kd_z\sin\theta d\theta$, and making use of Equations (1) and (3), this becomes

$$D=\frac{2\left(\sum_{-N_z}^{N_z} I_n\right)^2}{\frac{1}{kd_z}\int_{-kd_z-\alpha}^{kd_z-\alpha}\left(\sum_{-N_z}^{N_z} I_n e^{jn\psi}\right)\left(\sum_{-N_z}^{N_z} I_m e^{-jm\psi}\right)d\psi} \tag{24}$$

If d_z equals $\frac{\lambda}{2}$ (or any multiple thereof), this reduces very simply to

$$D=\frac{\left(\sum_{-N_z}^{N_z} I_n\right)^2}{\sum_{-N_z}^{N_z} I_n^2} \tag{25}$$

which is a most interesting formula in several respects. The directivity, as given by Equation (25), turns out to be a measure of the coherence of radiation from the linear array. The numerator is proportional to the total coherent field squared whereas the denominator is proportional to the sums of the squares of the individual fields from each element.

Furthermore, the directivity, as given by Equation (25), is seen to be independent of scan angle. On the face of it, this seems surprising, since we have already observed that the main beam broadens as it is scanned away from broadside, a manifestation which usually signifies lowered directivity. However, for a linear array, as the conical beam is scanned toward endfire, the cone tends to occupy a smaller solid angle in space, an effect which just cancels the beam broadening. This compensation holds until the beam approaches endfire, when another compensation takes over — the appearance of a second main beam at reverse endfire.

Whereas Equation (25) is independent of scan angle, it is not independent of current distribution. Using the Fourier series description of the excitation embodied in Equation (6), one finds that

$$\left(\sum_{-N_z}^{N_z} I_n\right)^2=(2N_z+1)^2\ a_o^2 \tag{26}$$

$$\sum_{-N_z}^{N_z} I_n^2=(2N_z+1)\sum_{-P}^{P} a_p^2 \tag{27}$$

so that

$$D=\frac{2N_z+1}{\sum_{-P}^{P}\left(\frac{a_p}{a_o}\right)^2} \tag{28}$$

For half-wave spacing, $L_z=(2N_z+1)\frac{\lambda}{2}$, so that Equation (28) can be rewritten

$$D=\frac{\frac{2L_z}{\lambda}}{1+2\sum_{p=1}^{P}\left(\frac{a_p}{a_o}\right)^2} \tag{29}$$

For element spacings in the range $\frac{\lambda}{2}\leqslant d_z\leqslant\lambda$, if L_z is held fixed, the directivity is found to be quite insensitive to element spacing. Since this is the range of element spacings which avoids either supergaining or multiple beams, we shall adopt Equation (29) as the expression for directivity of a linear array. Let us now interpret this equation for several cases.

Case 1: Uniform Distribution

Once again, this is the simplest case of all, and gives

$$D=\frac{2L_z}{\lambda} \tag{30}$$

which is sometimes referred to as the standard directivity (or gain). It is the maximum directivity which can be obtained from a linear array of length L_z, using an aperture distribution which has uniform progressive phase, and an element spacing of $\frac{\lambda}{2}$.

Case 2: Cosine-on-a-Pedestal Distribution

This is a special case of (29) in which only two terms appear in the denominator. It is more useful to display the normalized directivity, *D*, found by dividing (29) by (30). For this case,

$$D = \frac{1}{1+2\left(\frac{a_1}{a_0}\right)^2} \tag{31}$$

Since the practical range of $\frac{a_1}{a_0}$ extends from zero to one half, the normalized directivity extends from unity to two-thirds, and is independent of the size of the array.

Case 3: Chebyshev Distribution

Making use of the Fourier representation of a Chebyshev distribution, the directivity can be written

$$D = \frac{\frac{2L_z}{\lambda}}{1+\frac{2}{r^2}\sum_{p=1}^{N_z}\left[T_{2N_z}\left(u_0 \cos\frac{p\pi}{2N_z+1}\right)\right]^2} \tag{32}$$

a result which agrees with Stegen.[7]

Unlike the computation for beamwidth of a Chebyshev array, in which only the first two Fourier coefficients were significant, it develops that all the Fourier coefficients which appear in the denominator of (32) must be considered. Indeed, if the array becomes large enough, the sum of the squares of these Fourier coefficients becomes proportional to N_z, and thus the directivity tends to a limit. (cf. Appendix B for a proof of this statement).

It is a tedious computation to determine all the Fourier coefficients in (32), particularly for large arrays. Fortunately, this is not necessary. In Appendix C, it is shown that (32) can be written alternatively as

$$D = \frac{2r^2}{1+(r^2-1)f\frac{\lambda}{L_z}} \tag{33}$$

in which r is the main beam to sidelobe voltage ratio and f is the beam broadening factor. Equation (33) is quite accurate for large arrays and has the limit

$$D_{max} = 2r^2 \tag{34}$$

which is reached when $L_z \to \infty$ and which agrees with the result of Appendix B. Thus the maximum gain for a Chebyshev array is three db more than the sidelobe level. This means, for example, that if one wishes to design a linear array to have uniform sidelobes and a gain of 43 db, it is necessary also to design it to have sidelobes that are down at least 40 db. Actually, this maximum gain is approached rather rapidly at first, as L_z is increased, but then additional gain is bought very dearly in terms of increased array length. This point can be appreciated clearly by studying Figure 6, which is a plot of Equation (33) for various values of sidelobe level. An optimum gain (and thus array length) can be selected for a given sidelobe level by specifying a point on the appropriate curve of Figure 6 at which the curve has just barely begun to bend significantly. R. C. Hansen[8] has made an excellent study of such gain limitations for Taylor-type distributions and has come to similar conclusions.

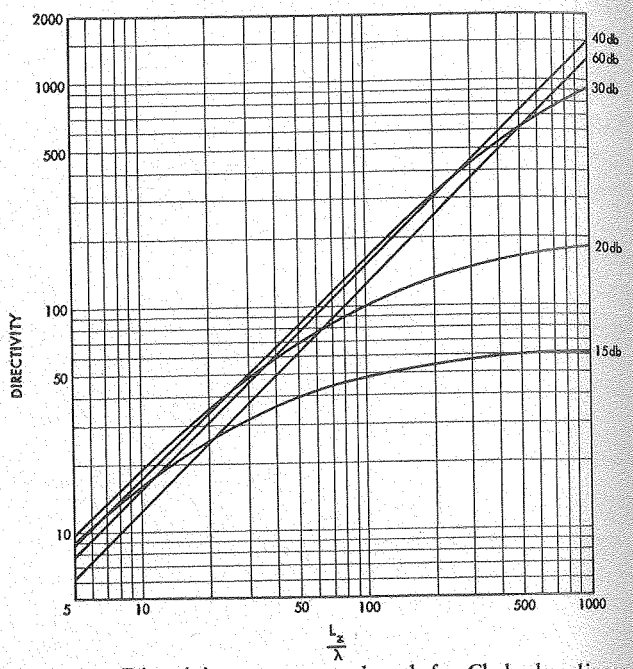

Figure 6 — Directivity versus array length for Chebyshev linear arrays.

This phenomenon of a gain limit was not observed for the cases of a uniform distribution and a cosine-on-a-pedestal distribution. Those distributions gave patterns with tapered sidelobes, and the Chebyshev feature of uniform sidelobes, while giving minimum beamwidth, is also responsible for the gain limitation. However, current antenna practice is to combine large arrays with low sidelobe levels, so this gain limitation is not so serious as to preclude the use of Chebyshev designs. For example, Figure 6 reveals that for arrays as long as one thousand wavelengths, very little bending has occurred in the curve for a 40 db sidelobe level.

Beamwidth and Directivity

Equations (9) and (29) reveal that for a linear array, both the beamwidth and the directivity depend linearly on the array length. Upon eliminating $\frac{L_z}{\lambda}$ from these two expressions, one obtains

$$D = \frac{1.77}{\textcircled{H}_0}\frac{f}{\left[\sum_{p=-P}^{P}\left(\frac{a_p}{a_0}\right)^2\right]} \tag{35}$$

in which $\textcircled{H}_0$ is the broadside beamwidth.

If the beamwidth is expressed in degrees instead of radians, and if the distribution is uniform, Equation (35) reduces to the simple relation

$$D = \frac{101.5}{\textcircled{H}_o} \qquad (36)$$

If a cosine-on-a-pedestal distribution is employed, the factor in brackets in (35) is a slowly-varying function of taper, only suffering a three per cent rise as a_1 increases to 0.25 a_o and only taking on a maximum increase of nine per cent at the extreme taper of $a_1 = 0.5\ a_o$. For a Chebyshev distribution, until an array length is reached at which the directivity begins to limit, the factor in brackets in (35) is unity. Thus Equation (36) is a good working relation between beamwidth and directivity for most useful excitations, and this can be rounded off by saying that the product of broadside beamwidth and directivity for a linear array is about one hundred.

Appendix A

Let

$$u_p = \frac{\pi d_z}{\lambda}\left(\cos\theta' - \cos\theta_o + \frac{p\lambda}{L_z}\right) \qquad (A\text{-}1)$$

so that Equation (7) can be written

$$A(\theta') = \sum_{-P}^{P} a_p \frac{\sin\ (2N_z+1)\ u_p}{\sin\ u_p} = \sum_{-P}^{P} a_p \frac{\sin\ [(2N_z+1)\ u_o + p\pi]}{\sin\ u_p}$$

$$= \frac{\sin\ [(2N_z+1)\ u_o]}{\sin\ u_o} \sum_{-P}^{P} a_p \cos p\pi \left[\frac{\sin\ u_o}{\sin\ u_p} - 1 + 1\right] \qquad (A\text{-}2)$$

For large arrays with conventional distributions, u_p and u_o are small angles and P is a small integer. Then (A-2) can be written

$$A(\theta') = (2N_z+1)\frac{\sin\ [(2N_z+1)\ u_o]}{(2N_z+1)\ u_o}\left\{a_o + \sum_{p=1}^{P} 2a_p \cos p\pi\right\}$$

$$-(2N_z+1)\frac{\sin\ [(2N_z+1)\ u_o]}{(2N_z+1)\ u_o}\sum_{p=1}^{P} 2a_p \cos p\pi \frac{p^2}{p^2-K^2} \qquad (A\text{-}3)$$

in which

$$K = \frac{L_z}{\lambda}(\cos\theta' - \cos\theta_o) \qquad (A\text{-}4)$$

But

$$A(\theta') = 0.707\ A(\theta_o) = 0.707 \sum_{-N_z}^{N_z} I_n = 0.707 \sum_{-P}^{P}\sum_{-N_z}^{N_z} a_p\ e^{jn\frac{2\pi p}{2N_z+1}}$$

$$A(\theta') = 0.707\ (2N_z+1)\ a_o \qquad (A\text{-}5)$$

Combining (A-3) and (A-5) gives

$$\frac{\sin K\pi}{K\pi}\left\{a_o + \sum_{p=1}^{P} 2a_p \cos p\pi\left[1 - \frac{p^2}{p^2-K^2}\right]\right\} = 0.707\ a_o$$

from which

$$\frac{\sin K\pi}{K\pi} = \frac{0.707}{1 - \sum_{p=1}^{P} \frac{2a_p}{a_o}\left(-1\right)^p \frac{K^2}{p^2-K^2}}$$

which can also be written

$$\frac{\sin K\pi}{K\pi} = \frac{0.707}{\sum_{-P}^{P} \frac{a_p}{a_o}\left(-1\right)^{p+1} \frac{K^2}{p^2-K^2}} \qquad (A\text{-}6)$$

Appendix B

Making use of the properties of the Chebyshev polynomials, we have

$$(2N_z+1)\ a_p = T_{2N_z}\left((u_o \cos\frac{p\pi}{2N_z+1}\right) = \cos 2N_z\ v_P \qquad (B\text{-}1)$$

in which v_p is defined by

$$\cos v_p = u_o \cos\frac{p\pi}{2N_z+1} \qquad (B\text{-}2)$$

and p is a large enough integer that v_p is real. (For practical distributions, $p \geq 3$ suffices.) Let

$$S = \sum_{p=3}^{N_z} (2N_z+1)^2 a_p^2 = \sum_{3}^{N_z} \cos^2 2N_z v_p$$

$$S = \sum_{3}^{N_z} \left(\frac{1}{2} + \frac{1}{2} \cos 4 N_z v_p \right) \qquad (B\text{-}3)$$

Since $u_o \cong 1$,

$$v_p = \frac{p\pi}{2N_z+1} + \delta_p \qquad (B\text{-}4)$$

in which δ_p is small, and tends to zero as $u_o \to 1$. Thus for large arrays, as p ranges from 3 to N_z, v_p ranges from a value close to zero to a value close to $\frac{\pi}{2}$, with the values of v_p being regularly spaced. Therefore the term

$$\sum_{3}^{N_z} \frac{1}{2} \cos 4 N_z v_p$$

is quite small, and, in (B-3),

$$S \to \frac{N_z}{2} \qquad (B\text{-}5)$$

Since, for a fixed sidelobe level, a_0, a_1, and a_2 remain constant as N_z is increased,[5] and since $(2N_z+1)a_o = r$, the main beam to sidelobe voltage ratio, Equation (28) yields the limit

$$D \to \frac{2N_z+1}{\frac{1}{r^2}(2)\left(\frac{N_z}{2}\right)} = 2r^2 \qquad (B\text{-}6)$$

Thus the limiting directivity of a Chebyshev linear array is governed by the sidelobe level.

Appendix C

For a large Chebyshev array, the denominator of Equation (23) can be approximated by assuming the main beam and each of the sidelobes to be a half-sinusoid in field distribution. The main beam has its maximum at θ_o and nulls at θ_2 and θ_1. In this range we assume

$$A(\theta) = r \cos \left[\frac{\theta - \frac{\theta_2+\theta_1}{2}}{\pi \frac{}{\theta_2-\theta_1}} \right] \qquad (C\text{-}1)$$

and determine a contribution to the denominator of (23) as

$$F_o = r^2 \sin \theta_o \int_{\theta_1}^{\theta_2} \cos^2 \left[\frac{\theta - \frac{\theta_2+\theta_1}{2}}{\pi \frac{}{\theta_2-\theta_1}} \right] d\theta \qquad (C\text{-}2)$$

in which $\sin \theta$ has been brought out in front of the integrand because a large array is assumed so that $\theta_2 - \theta_1$ is small and the variation in $\sin \theta$ is small. Equation (C-2) can be integrated easily, giving

$$F_o = r^2 \sin \theta_o \left(\frac{\triangle \theta_o}{2} \right) \qquad (C\text{-}3)$$

in which $\triangle\theta_o = \theta_2 - \theta_1$ is the angular width between nulls.

When a similar calculation is performed for one of the sidelobes, the only difference is that a unit amplitude replaces the amplitude r in (C-1). Thus Equation (23) can be written

$$D = \frac{2r^2}{r^2 \sin \theta_o \cdot \left(\frac{\triangle \theta_o}{2} \right) + \sum_{m}' \sin \theta_m \cdot \left(\frac{\triangle \theta_m}{2} \right)} \qquad (C\text{-}4)$$

in which $\triangle\theta_m$ is the angular width of the m^{th} sidelobe and the sum $\sum'$ extends over the entire angular region except for the portion occupied by the main beam. This can be rephrased as

$$D = \frac{4r^2}{(r^2-1)\sin \theta_o \cdot \triangle \theta_o + \sum_{m} \sin \theta_m \cdot \triangle \theta_m} \qquad (C\text{-}5)$$

in which the sum $\sum$ is over all space. For large arrays,

$$\sum_{m} \sin \theta_m \cdot \triangle \theta_m \cong \int_0^{\pi} \sin \theta \cdot d\theta = 2 \qquad (C\text{-}6)$$

Furthermore, the angular extent of the main beam is related to the half-power beamwidth by the expression

$$\triangle \theta_o \cong \frac{\text{Ⓗ}}{0.443} \qquad (C\text{-}7)$$

whereas the half-power beamwidth, using (14), is given by

$$\text{Ⓗ} = 0.886 \, f \frac{\lambda}{L_z} \csc \theta_o \qquad (C\text{-}8)$$

in which f is the beam broadening factor. Thus

$$\sin \theta_o \cdot \triangle \theta_o = 2f \frac{\lambda}{L_z} \qquad (C\text{-}9)$$

and therefore

$$D = \frac{2r^2}{(r^2-1) \, f \frac{\lambda}{L_z} + 1} \qquad (C\text{-}10)$$

References

1. Jordan, E. C., *Electromagnetic Waves and Radiating Systems*, Prentice-Hall, 1950, Chapter 12; and J. E. Eaton, L. J. Eyges, and G. G. MacFarlane, *Microwave Antenna Theory and Design*, McGraw-Hill, ed. S. Silver, 1949, Chapter 9.
2. Von Aulock, W. H., "Properties of Phased Arrays," *Proc. IRE*, Vol. 48, No. 10, Oct. 1960, pp. 1715-28.
3. King, M. J. and R. K. Thomas, "Gain of Large Scanned Arrays," *Trans. IRE*, Vol. AP-8, No. 6, Nov. 1960, pp. 635-6.
4. Silver, S., *Microwave Antenna Theory and Design*, McGraw Hill, 1949, p. 187.
5. Elliott, R. S., "An Approximation to Chebyshev Distributions," to appear in *AP Trans. of IEEE*.
6. Stegen, R. J., "Excitation Coefficients and Beamwidths of Tchebycheff Arrays," *Proc. IRE*, Vol. 41, Nov. 1953, pp. 1671-4.
7. Stegen, R. J., "Gain of Tchebycheff Arrays," *Trans. IRE*, Vol. AP-8, Nov. 1960, pp. 629-31.
8. Hansen, R. C., "Gain Limitations of Large Antennas," *Trans. IRE*, Vol. AP-8, Sept. 1960, pp. 490-5.

Part II of Dr. Elliott's paper, which will deal with planar array theory, will appear in the January issue of *the microwave journal*.